Structural and correlation effects in the itinerant insulating antiferromagnetic perovskite $NaOsO_3$

Myung-Chul Jung,[1] Young-Joon Song,[1] Kwan-Woo Lee,[1,2,*] and Warren E. Pickett[3,†]
[1]*Department of Applied Physics, Graduate School, Korea University, Sejong 339-700, Korea*
[2]*Department of Display and Semiconductor Physics, Korea University, Sejong 339-700, Korea*
[3]*Department of Physics, University of California, Davis, California 95616, USA*
(Received 3 October 2012; published 12 March 2013)

The orthorhombic perovskite $NaOsO_3$ undergoes a continuous metal-insulator transition (MIT), accompanied by antiferromagnetic (AFM) order at $T_N = 410$ K, suggested to be an example of the rare Slater (itinerant) MIT. We study this system using *ab initio* and related methods, focusing on the origin and nature of magnetic ordering and the MIT. The rotation and tilting of OsO_6 octahedra in the $GdFeO_3$ structure result in moderate narrowing of the bandwidth of the t_{2g} manifold but sufficient to induce flattening of bands and AFM order within the local spin density approximation, where it remains metallic but with a deep pseudogap. Including on-site Coulomb repulsion U, at $U_c \approx 2$ eV a MIT occurs only in the AFM state. Effects of spin-orbit coupling (SOC) on the band structure seem minor, as expected for a half-filled t_{2g}^3 shell, but SOC doubles the critical value U_c necessary to open a gap and also leads to large magnetocrystalline energy differences in spite of normal orbital moments no greater than 0.1 μ_B. Our results are consistent with a Slater MIT driven by magnetic order, induced by a combination of structurally induced band narrowing and moderate Coulomb repulsion, with SOC necessary for a full picture. Strong *p-d* hybridization reduces the moment, and when bootstrapped by the reduced Hund's rule coupling (proportional to the moment) gives a calculated moment of $\sim$1 μ_B, consistent with the observed moment and only a third of the formal d^3 value. We raise and discuss one important question: Since this AFM ordering is at $q = 0$ (in the 20 atom cell) where nesting is a moot issue, what is the microscopic driving force for ordering and the accompanying MIT?

DOI: 10.1103/PhysRevB.87.115119 PACS number(s): 71.20.Be, 71.30.+h, 71.27.+a, 75.50.Ee

I. INTRODUCTION

In condensed matter physics the origins of, and phenomena associated with, metal-insulator and magnetic transitions remain issues of fundamental interest, especially when they do not fit into a conventional mold. From this viewpoint, a few 5*d*-based oxides, including the osmate studied here, that display various high formal oxidation states are attracting great interest. They display an abundant variety of physical phenomena, including superconductivity, important effects due to large spin-orbit coupling (SOC), unconventional metal-insulator transitions (MIT) (the focus of this paper), and unusual magnetic behavior.

Within heptavalent Os^{7+} d^1 systems, the cubic double perovskite Ba_2NaOsO_6 is ferromagnetic with an unusually small magnetic moment while maintaining a cubic structure,[1] whereas the magnetic structures of the trigonal Na_3OsO_5 and Li_5OsO_6 and the double perovskite Ba_2LiOsO_6 are based on antiferromagnetic (AFM) order.[2–4] In the hexavalent d^2 systems, the double perovskite Ba_2CaOsO_6 is antiferromagnetic.[5] At the metallic $d^{2.5+}$ oxidation level, KOs_2O_6 in the β-pyrochlore structure shows superconductivity[6] at $T_c = 8$ K, whereas the triple perovskite $Ba_3LiOs_2O_9$ becomes AFM[7] at 13 K but shows significant reduction in the effective moment of 3.34 μ_B from the theoretical spin-only value of 4.78 μ_B, suggesting strong SOC effects. In a pentavalent d^3 system, the slightly distorted double perovskite Sr_2CrOsO_6 is a semimetallic ferrimagnet in which SOC plays an important part in the magnetic behavior by reducing the spin moment by 0.27 μ_B and inducing an orbital moment of 0.17 μ_B on the Os ion, decreasing the net moment by nearly a factor of 2.[8,9] Pentavalent $Cd_2Os_2O_7$, with its magnetic frustration on the pyrochlore Os sublattice, has been suggested to be an itinerant Slater insulator,[10] i.e., a MIT induced by antiferromagnetic ordering rather than by strong correlation effects.[11,12] Regarding Slater insulating states, d^5 Sr_2IrO_4, with a weakly canted antiferromagnetic MIT[13] at 250 K, has recently been characterized as a Slater insulator.[14] The character of the noncollinear ordered d^3 $Cd_2Os_2O_7$ is still under discussion.[15]

The orthorhombic perovskite $NaOsO_3$, also with pentavalent Os, synthesized by Shi *et al.*, undergoes a MIT coincident with antiferromagnetic ordering at the rather high temperature of $T_N = 410$ K with no evidence for any further structural distortion below 600 K.[16] The resistivity increases, and the Hall number decreases, by $\sim$3 orders of magnitude from T_N to 200 K and continued decreasing to 2 K, the insulating character becoming more accelerated below 25 K toward a strongly insulating ground state. The electronic contribution to the specific heat measurement vanished at low temperature, indicating a fully gapped Fermi surface. Due to this uncommon behavior, seemingly a continuously increase of gapping of the Fermi surface leading to a decrease and, finally, a vanishing of carriers, this system was argued to be the first example of the continuous MIT (the so-called Slater insulator with continuous opening of the AFM gap).

Recently, Calder *et al.* confirmed the continuous transition as a simultaneous change in magnetic and transport character.[17] The effective Curie moment of 2.71 μ_B observed by Shi *et al.* is reasonably consistent with a $S = 3/2$ moment, reduced (by 30%) by hybridization with oxygen and perhaps compensated somewhat by an orbital moment. This picture is one of high spin d^3 Os^{5+}.[16] Neutron power diffraction (NPD) measurements indicate G-type antiferromagnetism (G-AFM) with direction of moments alternating on neighboring Os ions,

but an Os *ordered moment* of only 1 μ_B.[17] This reduced value is difficult to reconcile with a $S = 3/2$ picture, since three dimensional arrays of large spins should not be subject to reduction by fluctuations. In the only previous theoretical work on $NaOsO_3$, Du *et al*. calculated a similar (even somewhat smaller) value from the sort of first-principles calculations we will describe and use below.[18] The NPD measurements show the spin oriented along the c axis without canting of the spins,[17] which provides additional information related to the impact of large SOC, one aspect that we want to investigate more thoroughly.

Du *et al*. obtained a magnetic ground state of the observed G-AFM type and provided a comparison of this state to other types of magnetic order that they could obtain in their calculations for $NaOsO_3$.[18] There remain several unresolved questions: (1) What is the origin and the nature of the AFM ordering, and what other states are energetically nearby? (2) Why is the ordered moment only 1 μ_B for pentavalent Os d^3? Is strong SOC a factor? (3) Why is this MIT continuous instead of the more common first-order type of MIT in transition metal oxides? (4) Does SOC perhaps play a more central role than is apparent from the results presented by Du *et al*.? The orientation of the moments (magnetocrystalline anisotropy) may provide useful conditions to address this question.

For another perovskite-based osmate Ba_2NaOsO_6, we observed strong interplay between correlation effects, small bandwidth, and strong SOC that are necessary to consider together to build an interpretation of the unusual features of that system,[1] which include that it is an uncommon *ferromagnetic* Mott insulator, it displays a very small ordered moment, and it remains cubic when it seems the d^1 configuration should favor at least a small Jahn-Teller distortion. In this paper, we address most of the questions we raised above, using first-principles spin-polarized calculations, including both correlation effects and SOC.

II. STRUCTURE AND METHODS

Shi *et al*. reported a highly distorted structure involving relative displacement of Na and O ions, leading to a $\sqrt{2} \times 2 \times \sqrt{2}$ quadrupled gadolinium orthoferrite type supercell (space group: *Pnma*, No. 62, as displayed in Fig. 1).[16] This large structure distortion is consistent with the small tolerance factor $t = 0.87$, using the Shannon ionic radius.[20] This $GdFeO_3$ structure type has been described in some detail by Pickett and Singh.[21] The lattice parameters are $a = 5.3842$, $b = 7.5804$, and $c = 5.3282$ (in units of Å), corresponding to the volume per formula unit (f.u.) of a cube with edge 3.788 Å. The atomic positions are given in Table I. This orthorhombic distortion leads to three somewhat different Os − O bond lengths, but all are close to 1.94 Å, resulting in a near-ideal aspect ratio of ∼1.002.[21] Thus the local structure is consistent with the t_{2g} orbitals being equally occupied (t_{2g}^3, $S = \frac{3}{2}$), retaining local cubic symmetry in the OsO_6 octahedron. The O − Os − O bond angles are 90.7°, 89.3°, or 89.1°, also indicating nearly ideal OsO_6 octahedra. However, the rotation and tilting of the octahedra are substantial. The O − Os − O axis tilts by 11° relative to the b axis and rotates by 9° in the a (or c) axis.

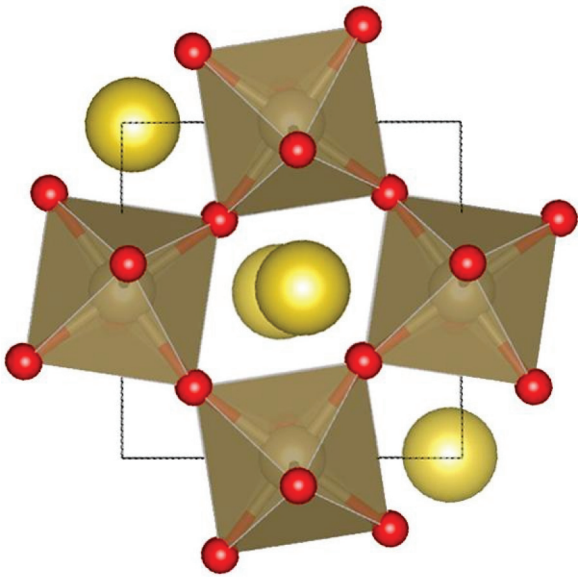

FIG. 1. (Color online) Distorted *Pnma* crystal structure of $NaOsO_3$, illustrating the $\sqrt{2} \times \sqrt{2}$ doubling cell in the a-c plane. There is also a doubling along the b axis due to tilting. The red (small) and the yellow (large) spheres indicate oxygen and Na atoms, respectively. This figure was produced by VESTA.[19]

In our work both SOC and correlation effects have been assessed, within LSDA + SOC, LDA + U, and LSDA + U + SOC approaches, implemented in two all-electron full-potential codes FPLO[22] and WIEN2K.[23] (The latter combination is available only in WIEN2K.) To include correlation effects in the half-filled t_{2g} shell, an effective on-site Coulomb repulsion $U_{\text{eff}} = U - J$ was used for the results we present, since experience has shown results very similar to those obtained from separate U and the Hund's exchange integral J inputs when a shell is half-filled. Convergence was checked up to a $14 \times 9 \times 14$ k-mesh of Brillouin zone sampling. In WIEN2K, the basis size was determined by $R_{\text{mt}} K_{\text{max}} = 7$, quite adequate for these atoms, and the APW radii were Na 2.14, Os 2.15, and O 1.4, in a.u.

III. MAGNETICALLY ORDERED ($T = 0$) PHASE

A. LSDA electronic structure

To begin, we compare electronic structures of the cubic and distorted phases. Within LSDA, the cubic phase has a higher energy by 378 meV/f.u. than the distorted structure in the nonmagnetic (NM) state, reflecting the strong lowering of energy by the distortion alone. The atom-projected densities of states (DOSs) in both phases are compared in the top panel

TABLE I. Atomic positions of atoms of $NaOsO_3$ in the *Pnma* (No. 62) structure, as experimentally observed.[16]

	Site symmetry	x	y	z
Na	4c	0.0328	$\frac{1}{4}$	–0.0065
Os	4b	0	0	$\frac{1}{2}$
Apical O	4c	0.4834	$\frac{1}{4}$	0.0808
Planar O	8d	0.2881	0.0394	0.7112

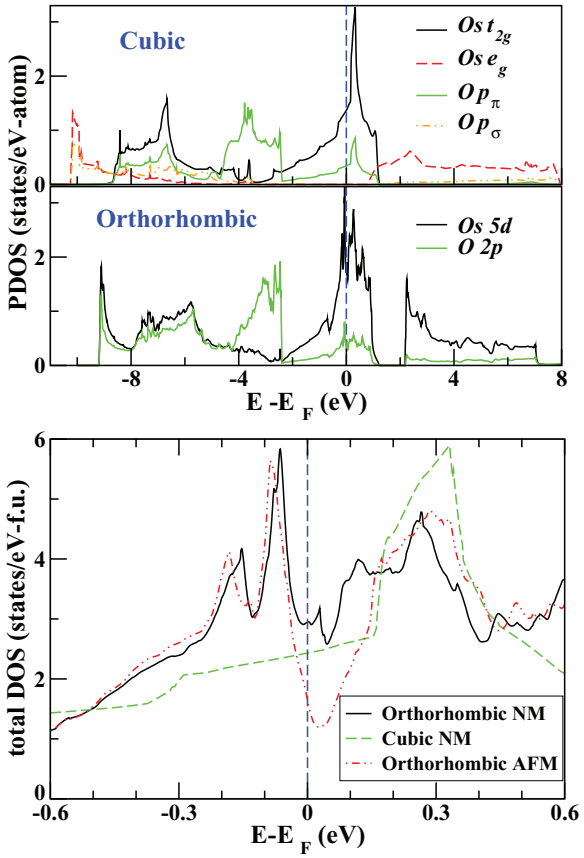

FIG. 2. (Color online) Top: Orbital-projected densities of states (DOSs) for Os $5d$ and O $2p$ in the cubic and distorted $Pnma$ crystal structures of nonmagnetic $NaOsO_3$. The distorted phase DOS shows more structure around the Fermi energy E_F, reflecting more flat bands that enhance magnetic instabilities. Bottom: Enlarged total DOSs of the nonmagnetic cubic phase and the distorted (orthorhombic) nonmagnetic and G-AFM phases, near E_F, which is set to zero. Notice that magnetic order strongly decreases $N(E_F)$.

of Fig. 2 and are consistent with those presented by Shi *et al.*[16] As discussed in Ru-based perovskites by Mazin and Singh,[24] the OsO_6 octahedra must be understood as oxygen-shared clusters. In the cubic phase, the t_{2g}-p_π antibonding ($pd\pi^*$) and bonding ($pd\pi$) states lie roughly in the –2.9 to 1.3 eV and of –8.7 to –4.7 eV regions, respectively. (The latter complex is typically neglected in characterizing the electronic structure and, in particular, the oxidation level, leaving the t_{2g}-based $pd\pi^*$ half filled as the physical t_{2g} bands.) Nearly pure p_π bands extend from –5 to –2.5 eV. The large orthorhombic distortion leads to narrowing bandwidth and enhancing the hybridization. The width of the $pd\pi^*$ manifold is reduced by 15%, and a hybridization gap of 1 eV appears between the $pd\pi^*$ manifold and the e_g-p_σ ($pd\sigma^*$) antibonding manifold.

The bottom panel of Fig. 2 compares the total DOS $N(E)$ of the NM cubic, NM distorted, and AFM distorted phases, near E_F. In the cubic phase, $N(E)$ varies smoothly very near E_F before giving way to a large narrow peak centered 0.3 eV above E_F. In the NM distorted phase, a sharp peak appears at –60 meV, and van Hove singularities appear just above E_F reflecting flat portions of bands that may encourage magnetic instability. However, our fixed spin moment calculations show

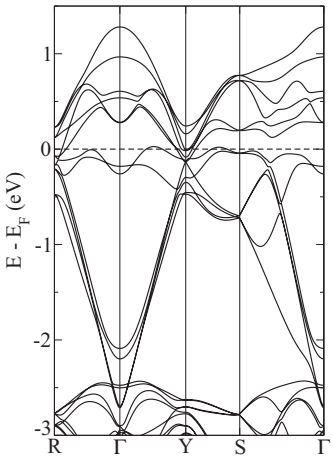

FIG. 3. AFM band structure in LSDA near E_F (zero of energy), which is crossed by the Os t_{2g} manifold. A deep and narrow pseudogap is centered at E_F. The Os e_g bands lie higher, above the range of this figure, while the O $2p$ bands lie below –2.5 eV. In units of $(\pi/a,\pi/b,\pi/c)$ the symmetry points shown are $R = (111)$, $\Gamma = (000)$, $Y = (010)$, and $S = (110)$.

no evidence of any nearby stable or metastable ferromagnetic state.[25] In addition to sharp peaks on either side of E_F, the AFM DOS of the distorted phase shows a deep pseudogap just above E_F, suggesting that applying U to the Os $5d$ states at this band filling will open a gap.

Within LSDA, the AFM state with an Os spin moment of 0.6 μ_B has a *very slightly lower energy* of 3 meV/f.u. than NM in the experimentally observed structure. The local moment of oxygens is negligible due to their symmetric placement between antialigned Os moments. This degeneracy (within a fraction of $k_B T_N$/Os) rationalizes the existence of a magnetic ordering transition in $NaOsO_3$. Figure 3 presents the enlarged LSDA band structure, showing only the Os t_{2g} (i.e., $pd\pi^*$) manifold with the width $W = 3.5$ eV. The deep pseudogap in the DOS of Fig. 2 results from an incipient gap formation arising as a combination of the distorted lattice and AFM order. The valence (occupied) band complex has become nearly disjoint from the conduction (unoccupied) bands in nearly the entire zone, with slight overlap remaining at the Y and R points. The top two occupied bands are quite flat, accounting for the sharp peaks at –0.1 and –0.2 eV as shown in the bottom panel of Fig. 2.

B. Conditions for antiferromagnetic ordering

To probe the effects of the structural geometry on the AFM state, we varied both the volume and the angles of the OsO_6 octahedral rotation. In the cubic structure with the same volume as the experimentally observed structure, no AFM order could be obtained. To check further for magnetic order in the cubic phase, the lattice parameter of the cubic phase was varied in the range of ±3%. No magnetic order was obtained, indicating that the AFM order is not induced by simple variation of the Os − Os distance. Also, as expected, no AFM order is induced by Na displacement.

Next we varied the two structural angles individually. At a critical tilt of $\theta_c = 3^\circ$, a hybridization gap between $pd\pi^*$ and $pd\sigma^*$ manifolds appears, accompanied by AFM ordering

with an Os moment of 0.26 μ_B. Somewhat unexpectedly, this moment remains unchanged up to $\theta = 11^\circ$, the observed tilt angle. When rotating the octahedra by ϕ, AFM with $M_{\rm Os} = 0.13\ \mu_B$ appears at $\phi_c = 9^\circ$, where the overlap between the $pd\pi^*$ and $pd\sigma^*$ manifolds becomes very small. In all cases the opening of a hybridization pseudogap around the Fermi level accompanies the AFM order, establishing a close connection in this compound between structure and magnetic order.

C. Metal-insulator transition versus $U_{\rm eff}$

Now we focus more closely on correlation effects beyond LSDA on the AFM state in the observed distorted structure, by applying the on-site Coulomb repulsion $U_{\rm eff}$ to Os ions using the LDA + U method. As might be anticipated from the pseudogap at E_F at the required band filling, a gap opens for $U_{\rm eff}$ as small as 1 eV. The Os local moment is 1.0 μ_B, consistent with the experimentally observed value.[17] This value is nearly unchanged when SOC is included (see below). Considering $5d^3$ Os^{5+} ions, the naive expectation based on a localized $5d$ orbital is that orbital and spin ordering of $t_{2g}^{2\uparrow} t_{2g}^{1\downarrow}$ (corresponding to a highly unusual spin density) would be required to obtain this reduced value of moment. In the insulating state, the spin density, however, assumes a local cubic symmetry dimpled dice shape, shown in Fig. 4, which confirms equal occupation of the t_{2g} orbitals.

At $U_{\rm eff}^c$, the d occupation matrix substantiates this conclusion. The majority t_{2g} orbitals are almost equally occupied at about $0.7e$ per orbital, substantially reduced from the formal value of unity. The majority e_g and all the minority d orbitals, which are formally unoccupied, each have occupation of about $0.3e$ per orbital, reflecting substantial p-d hybridization and indicating a strong deviation from the conventional ionic d^3 viewpoint. In total, there are 4.3 electrons throughout the d orbitals, instead of the formal value, 3. This "discrepancy" is not so surprising, as it is widely recognized that an actual charge on d cations differs from the formal charge, sometimes[26] by a factor of 2. For Os here, the formal charge of +5 is contrasted with an actual charge of around +3.7. The reduction by a factor of 3 of the formal moment is a more notable feature and, unlike the case of Ba_2NaOsO_6 where the moment is also vastly reduced,[9] here it is unrelated to SOC. $NaOsO_3$ is a case of an insulating transition metal oxide where the formal charge (oxidation state) picture is murky at best,

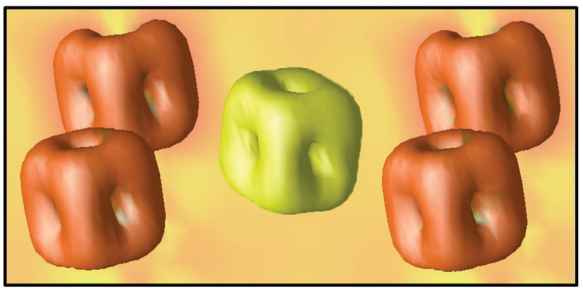

FIG. 4. (Color online) Spin density plot of Os ions in the a-c plane, with isosurface at 0.13 $e/\text{Å}^3$. This is obtained in LDA + U at $U_{\rm eff} = 1$ eV, where this system becomes insulating, and reflects locally cubic symmetry. The different color indicates the opposite spin orientation in the G-AFM alignment.

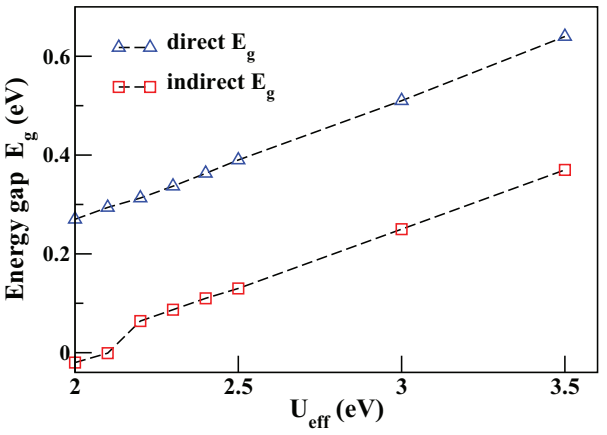

FIG. 5. (Color online) Direct and indirect gap vs effective U in LSDA + U + SOC calculations. Below the critical value of $U_{\rm eff}^c = 2.2$ eV, the indirect gap becomes negative, i.e., the bands are semimetallic.

consistent with the itineracy evident in the electronic structure and apparently in the MIT as well.

Figure 5 shows change in the direct and indirect gaps due to varying $U_{\rm eff}$. In the distorted structure and including SOC, an energy gap opens only at $U_{\rm eff}^c = 2.2$ eV.[27] Above $U_{\rm eff}^c$, both gaps increase linearly at a rate of 0.16 eV/eV, with the difference of 0.3 eV independent of $U_{\rm eff}$. Below $U_{\rm eff}^c$, a negative indirect gap (not shown) results due to significant lowering of the bottom of the conduction band at the Y point, though the direct gap is already established (the occupied and unoccupied bands are disjoint). This feature may be related with the proposal of a continuous transition in opening an energy gap, as discussed in another osmate $Cd_2Os_2O_7$ by Shinaoka *et al.*[12] Considering a likely $J \approx 0.5$ eV, $U^c \approx 2.7$ eV $\sim W$ suggests, for this multiband system, that a Mott transition is not the appropriate picture for this continuous MIT.

The corresponding band structure at $U_{\rm eff}^c$ is displayed in Fig. 6. The SOC splitting is about 0.2 eV at the Γ point. An unusual outcome of the structural distortion is that the top of the valence bands is nearly flat, reflected in the step increase

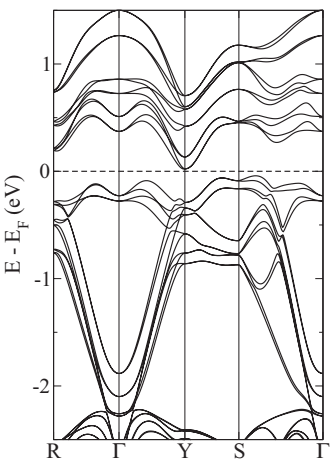

FIG. 6. Enlarged AFM band structure of Os t_{2g} manifold at $U_{\rm eff} = 2.2$ eV in LSDA + U + SOC. A gap opens at $U_{\rm eff} = 1$ eV in the LDA + U, but $U_{\rm eff} = 2.2$ eV is required when SOC is included.

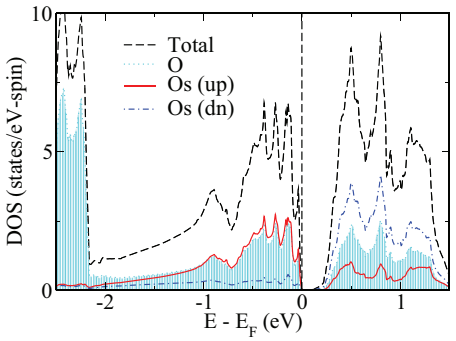

FIG. 7. (Color online) AFM total and atom-projected DOSs, including primarily the Os t_{2g} manifold, within LSDA + U + SOC at $U_{\rm eff}^{c} = 2.2$ eV in the distorted structure. In the occupied states below E_F, the unpolarized O $2p$ DOS mirrors closely the majority Os t_{2g} DOS. The result is a greatly reduced spin moment on the Os ion (see text).

in the valence band DOS evident in Fig. 7, and provides a two-dimensional character to the low-energy phase space. We also point out that the dispersion is very similar above and below E_F, relevant information for yet-to-be-done optical experiments since the k-conserving joint DOS may be sharply peaked at the onset of absorption. Within LSDA + U + SOC as in LSDA, the AFM state is nearly degenerate with the NM state. The fact that neither state is energetically favored is consistent with the finite temperature transition between the two states.

The value of U appropriate for $NaOsO_3$ has already been mentioned in the literature, in addition to the conclusion $U \sim 2$ eV of Du *et al.* that is nearly identical to ours. Calder *et al.* reported data on magnetic x-ray resonant scattering (MXRS) with interpretation from x-ray absorption near edge spectra (XANES) obtained from Joly's finite difference code.[28] They obtained a better correspondence using $U = 0$ than with nonzero U. We think there is no direct contradiction. In their work they are dealing with resonant transitions between deep $2p_{1/2}$ and $2p_{3/2}$ levels and unoccupied $5d$ states. In our work, based on the self-consistent LDA + U method, the effect of U is to increase the separation of occupied $5d$ bands and unoccupied $5d$ bands, which is a different issue involving a U in a different manner.

D. Additional effects of spin-orbit coupling

As discussed for several decades, t_{2g} orbitals, when split off from the e_g orbitals by the crystal field, form a representation of an angular momentum of $L = 1$.[1] In the spherical Hund's rule limit the total angular momentum is zero for a high spin t_{2g}^3 system. Especially in this locally cubic geometry and half filling, the orbital moment should be small. As shown in Table II, inclusion of SOC leads to an orbital moment antialigned with the spin moment and with magnitude no larger than 0.1 μ_B. Thus, in the insulating state, the net moment remains about 1 μ_B, consistent with the experimentally observed value[17] and relatively insensitive to $U_{\rm eff}$ in the range studied here (see Table II).

We have calculated total energies with LDA + U + SOC with four spin orientations ⟨100⟩, ⟨010⟩, ⟨001⟩, and ⟨111⟩ to determine the easy axis. As observed by Calder *et al.*,[17] ⟨001⟩ is the easy axis. Along ⟨010⟩, both spin and orbital moments increase by 10% in magnitude, but the energy cost is large, 474 meV/f.u., despite some additional Hund's coupling energy. Along ⟨111⟩, the spin moment is enhanced to 1.25 μ_B while the energy is higher by 51 meV/f.u. Consistent with the similarities between the a and c axes (the octahedron rotation is around the b axis) the energy difference is small, only 5 meV/f.u.

TABLE II. Local moments of Os in the distorted AFM $NaOsO_3$ in LSDA + U + SOC calculations with the ⟨001⟩ quantization axis. The moments of oxygens are at most 0.01 μ_B/atom.

$U_{\rm eff}$ (eV)	State	Spin	Orbital
1	Metallic	0.69	− 0.050
2	Semimetallic	1.03	− 0.085
2.5	Insulating	1.13	− 0.097
3.0	Insulating	1.22	− 0.106

IV. FINITE TEMPERATURE; METAL-INSULATOR TRANSITION

Approached from high temperature, a continuous MIT occurs at the point where the spin-symmetric phase becomes unstable to magnetic order, which is AFM order in the case of $NaOsO_3$. In Slater-type (itinerant) transitions, ordering conventionally is driven by Fermi surface (FS) nesting, as in the classic case of chromium. The common picture for a Slater MIT is that a spin density wave (SDW) gaps at least a portion of the FS, and the increasing amplitude of the SDW destroys more and more of the FS as the temperature is lowered. The specific heat data for $NaOsO_3$ indicate the FS is completely gone as $T \to 0$. The resistivity data strongly suggests it has been effectively destroyed at intermediate temperature, since the magnitude and temperature coefficient reflect insulating behavior even as spin-fluctuation scattering has began to be frozen out by the magnetic order (which, in itself, should *lower* rather than increase the resistivity), and the strongly decreasing Hall coefficient is consistent with rapidly shrinking FSs. In this section we, first, discuss the electronic structure in the (high temperature) nonmagnetic metallic state, albeit without consideration of the thermal broadening and the lattice dynamical and spin fluctuation scattering that may be necessary for a detailed picture. We then provide a scenario for the MIT that is consistent with observations and what is understood about the electronic structure.

A. Electronic structure in the nonmagnetic phase

The LDA and LDA + SOC band structures without magnetic order are displayed together in Fig. 8. We have checked that including $U_{\rm eff}$ in this nonmagnetic phase leads to negligible effect, as is commonly observed. In the previous section we established that SOC has relatively little impact on the bands in the AFM phase, displaying its main impact by its seeming competition with correlation effects so the correlation strength necessary to open the gap (within the AFM phase) is doubled to ∼2 eV. Near E_F, the effect of SOC on the

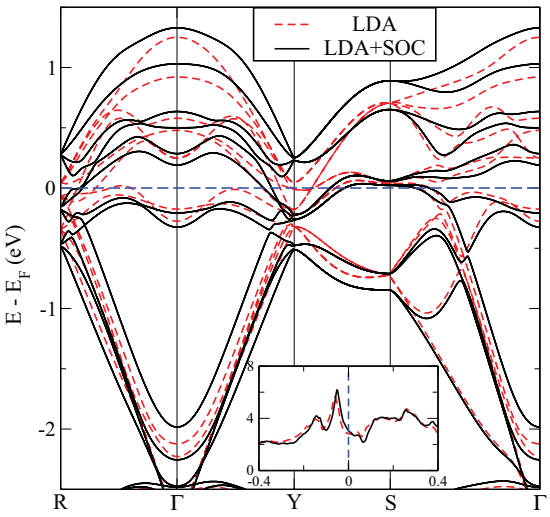

FIG. 8. (Color online) Enlarged view of the nonmagnetic t_{2g} band structures appropriate to the high-T nonmagnetic phase in LDA (red dashed lines) and LDA + SOC (black solid line). Including U makes negligible difference. Inset: Nonmagnetic total DOSs in LDA (red dashed lines) and LDA + SOC (black solid lines) near E_F (in states/eV-f.u.).

band structure (Fig. 8) in the high-T phase again seems minor, but it is clearly visible at symmetry points (Y, S) where it removes degeneracies and splits bands. Moreover, the effect on the DOS is minor, as is clear from the inset of Fig. 8. With or without SOC, the Fermi level DOS $N(E_F)$ ≈ 3 states/eV-f.u. for both spins, corresponding to a linear specific heat coefficient $\gamma = 7$ mJ/mol-K^2. This standard metallic value is corroborated by large FS sheets, which we now discuss.

Because the topology of the FSs is central to a SDW transition, we display FSs without and with SOC in Fig. 9. The small shifts in band energies due to SOC that can be seen in Fig. 8 are translated by the small velocities into considerable changes in the complex multisheeted FSs, with some of the clearest changes occurring around the symmetry points. The FSs retain to some extent an approximate fourfold symmetry in the a-c plane (x-y plane in Fig. 9), which, of course, is not a true symmetry of the $Pnma$ structure but is useful to recognize. There are both electron- and hole-type surfaces, making the magnitude of the Hall coefficient difficult to interpret.

B. Comments on the metal-insulator transition

Most theoretical work on AFM transitions in metals, including very recent ones, focus either on FS nesting (Cr is the classic example) or FS "hot spots" involving band and FS folding due to the finite-q order that set in at the transition. In the first case the nested sections of FS become gapped, while in the second case the FS also reconstructs but in a less obvious manner. For example, Sachdev *et al.*[29] review the latter scenario and provide evidence of a breakdown of fermionic quasiparticle excitations at the transition, and a FS reconstruction from large to small surfaces that have been discussed for many years in the high-temperature superconducting cuprates.

Both the nesting scenario and the hot-spot scenario of the continuous Slater transition to an AFM incurs difficulty

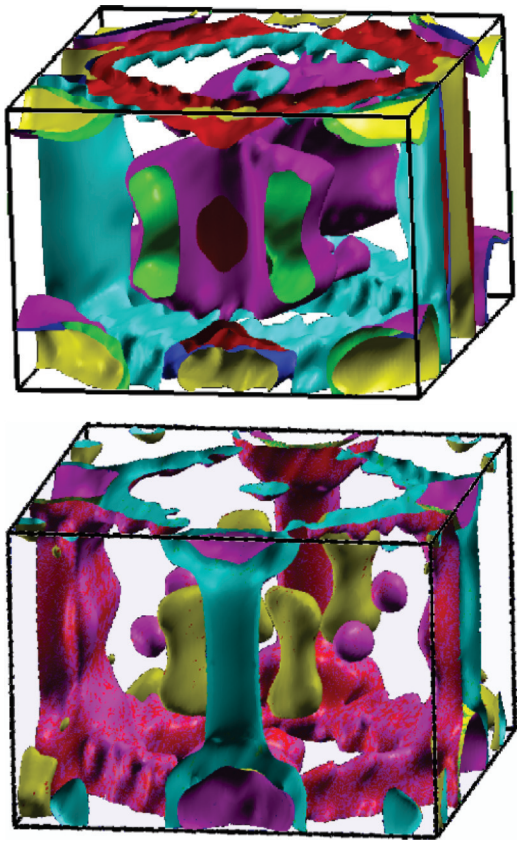

FIG. 9. (Color online) Fermi surfaces of LDA (top) and LDA + SOC (bottom) in the nonmagnetic state. The Y point is at the center of the front face. In both cases complex multisheeted surfaces exist, but SOC results in substantial rearrangement in Fermi surfaces.

in $NaOsO_3$, because it is a $q = 0$ ordering for which both scenarios, which focus on a nonzero wave vector Q_{AF}, become moot. This situation can arise, and not uncommonly, in crystal structures with more than one magnetic ion of a given type. In $NaOsO_3$, the four symmetry-related Os ions in the $GdFeO_3$ distorted lattice devolve into two pairs, with spins in opposite directions. Interestingly, the original exposition by Slater[10] did not involve finite-q physics in any explicit manner. His picture, based on spin-unrestricted Hartree-Fock theory, was that AFM ordering would introduce new Fourier components in the (spin-dependent) potential, leading to new gaps in the band structure that could well appear at the Fermi level, especially in stoichiometric compounds where there is the likelihood that bands can be completely occupied or completely unoccupied. If the new gaps appear at a zone boundary, it will be energetically favored to double the periodicity, as in the simplest picture of SDW order. Yet if the new gaps appear only at $q = 0$ (no cell doubling), the band structure may still become gapped in spite of the lack of any extension of periodicity.

The effect of AFM ordering in $NaOsO_3$ on the electronic structure can be seen by comparing the metallic bands of the nonmagnetic high-T phase in Fig. 8 (solid lines) with the AFM insulating bands in Fig. 6. New Fourier components of the potential separate the bands strongly at zone boundary symmetry points (*viz.*, R, Y, S) and at the zone center the bands are already split. Slater also tied this type of ordering to bonding-antibonding band formation, which provides a band

energy (bonding energy) gain in addition to the Hund's rule (magnetic) gain in energy.

A rudimentary picture that is consistent with data and with this understanding of the electronic structure can be assembled. Already at high T the strongly distorted, four f.u. per primitive cell, structure is dictated by the tolerance ratio of 0.87. The distortion leaves flat bands at and near the FS, which is large and multisheeted. At T_N, magnetic order sets in and the metallic band structure begins to morph continuously toward the $T = 0$ AFM insulating band structure. The FSs, both electron and hole types, begin to shrink in volume and vanish one by one, until no FS remains. The change from the metallic to the insulating band structure should be monotonic in, and nearly proportional to, the magnetic order parameter. The magnetic order parameter measured by Calder *et al*. was provided only down to $\sim 0.85\ T_N$,[17] so it is not possible to estimate when the last FS may be expected to disappear. As mentioned earlier, thermal smearing and lattice and spin fluctuations will complicate a detailed picture. One loose end in this picture is the apparent discontinuity—a jump by roughly 50%—in the paramagnetic susceptibility[16] just below T_N.

Without a Fermi surface or hot-spot origin, the mechanism of G-type ordering is not clear and was not addressed by Du *et al*. in their theoretical study of magnetic ordering.[18] Since G-type ordering is common in perovskite transition metal oxides, it seems likely this ordering represents an emergence of the nearest-neighbor AFM coupling commonly occurring in perovskites, in spite of the apparent itineracy in the electronic structure and the collapse of the d^3 valence state picture.

V. SUMMARY

Our results have clarified a number of features of $NaOsO_3$, and the questions posed in Sec. I. First, a combination of the distortion of the perovskite structure and moderate correlation effects is responsible for both antiferromagnetism and the insulating gap in the ground state. Our calculations account naturally for the factor of three reduction in the observed moment ($1\ \mu_B$) relative to the ideal t_{2g}^3 value, due to very strong hybridization with the O $2p$ orbitals that render the conduction states, and the magnetism, itinerant in nature. The oxygen ions, being coordinated with two Os ions with antialigned spins, are unpolarized by (approximate) symmetry. The calculated energetics, with small energy difference between the magnetic and nonmagnetic states, is also consistent with a Slater-type metal-to-insulator transition to an AFM state. Moreover, the simplest specification of a Mott insulator is one in which the insulating state does not depend on magnetic order. In $NaOsO_3$ all the evidence indicates that magnetic order is *necessary* for insulating behavior. Because of the itinerant nature of the moment, a Heisenberg model cannot provide a representation which could then be applied to predict the Néel temperature.

Spin-orbit coupling, often a dominant force in $5d$ metal oxides, has a more modest effect in this compound. While it affects the band structure enough that the effective coupling strength U_{eff} is increased from 1 to 2.2 eV, it is in itself ineffective in decreasing the local moment. The strong moment reduction (from a localized high-spin t_{2g} picture of $3\ \mu_B$) is due to strong hybridization with O $2p$ orbitals—that is, itineracy—which is itself affected by the distortion. The minor importance of SOC is consistent with the finding of Calder *et al*. that x-ray resonant photoelectron spectra show only minor effect of SOC.[17]

Though $3d$ perovskite oxides have been studied extensively for decades, their $5d$ counterparts are relatively new to detailed inspection of their properties and the underlying mechanisms. Our results for $NaOsO_3$ will help to provide a basis for understanding the distinctions in the physics of $5d$ versus $3d$ (and $4d$) oxides.

ACKNOWLEDGMENTS

This research was supported by the Basic Science Research Program through the NRF of Korea under Grant No. 2012-0002245. W.E.P was supported by the DOE under Grant No. DE-FG02-04ER46111.

*mckwan@korea.ac.kr
†pickett@physics.ucdavis.edu

[1] K.-W. Lee and W. E. Pickett, Europhys. Lett. **80**, 37008 (2007).
[2] K. M. Mogare, W. Klein, H. Schilder, H. Lueken, and M. Jansen, Z. Anorg. Allg. Chem. **632**, 2389 (2006).
[3] S. Derakhshan, J. E. Greedan, and L. M. D. Cranswick, Phys. Rev. B **77**, 014408 (2008).
[4] K. E. Stitzer, M. D. Smith, and H. zur Loye, Solid State Sci. **4**, 311 (2002).
[5] K. Yamamura, M. Wakeshima, and Y. Hinatsu, J. Solid State Chem. **179**, 605 (2006).
[6] S. Yonezawa, Y. Muraoka, Y. Matsushita, and Z. Hiroi, J. Phys.: Condens. Matter **16**, L9 (2004).
[7] K. E. Stitzer, A. El Abed, M. D. Smith, M. J. Davis, S. J. Kim, J. Darriet, and H. C. zur Loye, Inorg. Chem. **42**, 947 (2003).
[8] Y. Krockenberger, K. Mogare, M. Reehuis, M. Tovar, M. Jansen, G. Vaitheeswaran, V. Kanchana, F. Bultmark, A. Delin, F. Wilhelm, A. Rogalev, A. Winkler, and L. Alff, Phys. Rev. B **75**, 020404(R) (2007).
[9] K.-W. Lee and W. E. Pickett, Phys. Rev. B **77**, 115101 (2008).
[10] J. C. Slater, Phys. Rev. **82**, 538 (1951).
[11] D. Mandrus, J. R. Thompson, R. Gaal, L. Forro, J. C. Bryan, B. C. Chakoumakos, L. M. Woods, B. C. Sales, R. S. Fishman, and V. Keppens, Phys. Rev. B **63**, 195104 (2001).
[12] H. Shinaoka, T. Miyake, and S. Ishibashi, Phys. Rev. Lett. **108**, 247204 (2012).
[13] M. K. Crawford, M. A. Subramanian, R. L. Harlow, J. A. Fernandez-Baca, Z. R. Wang, and D. C. Johnston, Phys. Rev. B **49**, 9198 (1994).
[14] R. Arita, J. Kuneš, A. V. Kozhevnikov, A. G. Eguiluz, and M. Imada, Phys. Rev. Lett. **108**, 086403 (2012).
[15] J. Yamaura, K. Ohgushi, H. Ohsumi, T. Hasegawa, I. Yamauchi, K. Sugimoto, S. Takeshita, A. Tokuda *et al*., Phys. Rev. Lett. **108**, 247205 (2012).
[16] Y. G. Shi, Y. F. Guo, S. Yu, M. Arai, A. A. Belik, A. Sato, K. Yamaura, E. Takayama-Muromachi, H. F. Tian, H. X. Yang, J. Q. Li, T. Varga, J. F. Mitchell, and S. Okamoto, Phys. Rev. B **80**, 161104(R) (2009).

[17] S. Calder, V. O. Garlea, D. F. McMorrow, M. D. Lumsden, M. B. Stone, J. C. Lang, J.-W. Kim, J. A. Schlueter, Y. G. Shi, K. Yamaura, Y. S. Sun, Y. Tsujimoto, and A. D. Christianson, Phys. Rev. Lett. **108**, 257209 (2012).
[18] Y. Du, X. Wan, L. Sheng, J. Dong, and S. Y. Savrasov, Phys. Rev. B **85**, 174424 (2012).
[19] K. Momma and F. Izumi, J. Appl. Crystallogr. **41**, 653 (2008).
[20] http://www.webelements.com.
[21] W. E. Pickett and D. J. Singh, Phys. Rev. B **53**, 1146 (1996).
[22] K. Koepernik and H. Eschrig, Phys. Rev. B **59**, 1743 (1999).
[23] K. Schwarz and P. Blaha, Comput. Mater. Sci. **28**, 259 (2003).
[24] I. I. Mazin and D. J. Singh, Phys. Rev. B **56**, 2556 (1997).
[25] K. Schwarz and P. Mohn, J. Phys. F **14**, L129 (1984).
[26] Y. Quan, V. Pardo, and W. E. Pickett, Phys. Rev. Lett. **109**, 216401 (2012).
[27] In Ref. 18, Du *et al*. quoted $U^c = 2$ eV, without mentioning J explicitly. Considering that they also used WIEN2K, this value seems to be $U^c_{\rm eff}$, which is consistent with our results.
[28] Y. Joly, Phys. Rev. B **63**, 125120 (2001).
[29] S. Sachdev, M. A. Metlitski, and M. Punk, J. Phys.: Condens. Matter **24**, 294205 (2012).